BEAM SIMULATIONS IN LIPAc

Akihiko Mizuno*[1], Jibong Hyun, Kouki Hirosawa, Kai Masuda, QST
Pau González, Hervé Dzitko, F4E
Nicolas Chauvin, Université Paris-Saclay CEA
Luca Bellan, INFN/LNL
[1]also at JASRI

Abstract

LIPAc is the prototype hadron accelerator for IFMIF, a neutron source for testing new materials in future fusion reactors, so a very high beam current is necessary and a loss-free design is crucial. In this respect, pre-experimental beam simulations are very important for setting device parameters. By the summer of 2024, we were able to confirm that the simulation and experimental results matched for beam size very well and achieved a beam duty cycle of 8.75 % with current of 119 mA. In the presentation, we report on reliability of simulation and how the calculated and measured results matched up. But we also observed some activation at several locations, which may be due to the beam halo. We also report on simulation studies of the halo.

INTRODUCTION

LIPAc is the prototype hadron accelerator for IFMIF, a neutron source for testing new materials in future fusion reactors, under BA agreement between EURATOM and Japan govenment, at Rokkasho, Aomori.

Figure 1 shows the schematic diagram of the LIPAc as of summer in 2024.

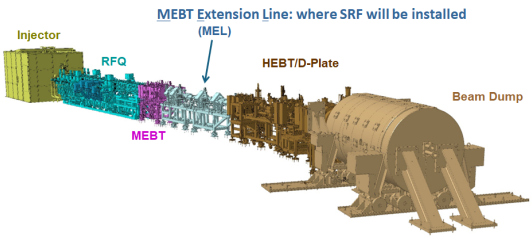

Figure 1: The schematic diagram of the LIPAc for Phase B+.

It is composed of the injector part and the 10-m-long RFQ. The energy is up to 5 MeV at exit of the RFQ. After the RFQ, there are 2 bunchers, and the beam passes through MEBT, MEL, and HEBT and is then bent 20 degrees by a bending magnet before being injected into the beam dump. There are 17 quadrupole magnets from the RFQ to the beam dump. The experiment is being carried out in stages, with Phase B+ testing being successfully completed in the summer of 2024 with the configuration shown in Fig. 1. Currently, construction is underway to install a superconducting accelerating cavity (SRF) with energies up to 9 MeV in the MEL section, and experiments are planned to resume in 2027 as Phase C.

* mizuno.akihiko@qst.go.jp

The current is 125 mA with deuteron and we are aiming for CW operation. Therefore, the operations without beam losses are very important to avoid activation or heat accidents. Also quenching of the SRF must be avoided. From these respects, it is very important to perform a beam simulation in advance and determine the parameters of devices.

In this paper, we describe beam simulations in the LIPAc project.

SIMULATION CODE

It has been agreed in our project that we use TraceWin [1] as beam tracking simulation tool, which is developed by Saclay CEA. It is a PIC code. The advantage is that the calculation speed is fast. The elapsed time from the exit of the RFQ to the beam dump is approximately several minutes with particle number of ~ 10^6. It features a beam matching function that automatically determines device parameters to set the transverse beam sizes and divergences at specific points, and it is very useful. Also it can perform error calculations, which is tracking ~ 10^4 times with varying magnet current, RF powers and alignment error of the devices in the limited range. It is useful for checking the beam losses at specific points.

Figure 2 shows one of the result of matching sequence. The beam has some space between the ducts and there are no beam losses. Note that the beam diameter grows up at the beam dump to clear the heat condition.

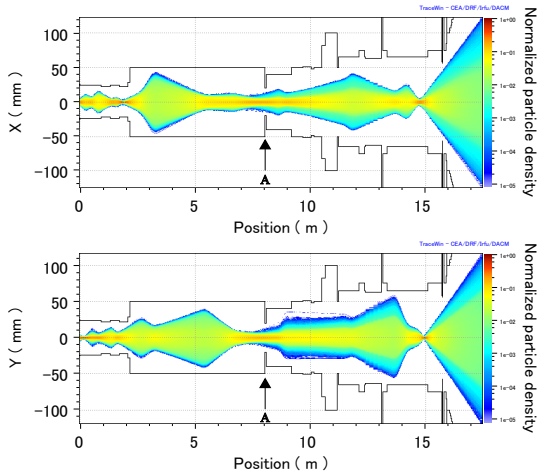

Figure 2: Typical plots of beam profile from the RFQ exit to the beam dump. The shading represents the charge density. Point A is used in Fig. 14.

SIMULATION CODE RELIABILITY

To evaluate reliability of the code is very important. Figure 3 shows time evolution of transverse beam sizes calculated by TraceWin and Point-to-Point code [2] which is developed by the author. The power of the first buncher is de-turned and the second buncher is powered, the current is 125 mA. Numbers of the particle are 157316 in TraceWin and 78655 in Point-to-Point code. We aim for CW beam operation, so the beam forms bunch trains rather than a single bunch, and in TraceWin the bunches are always calculated as bunch trains. Therefore also in Point-to-Point code, we simulated bunch trains by positioning two bunches before and after the main bunch as shown in Fig. 4. There is a bending magnet from $z = 12.4$ m to $z = 13$ m but it is not included in Point-to-Point code calculations, therefore beam sizes in x direction are slightly different for the two codes after the bending magnet. Except for that, the beam sizes match very well between the two codes, despite the overlap of adjacent bunches downstream.

Point-to-Point code is simple code which calculates electromagnetic field from the point charge and tracks each particle by 4th-order Runge-Kutta method, and the space charge calculation techniques are completely different in the two codes. Therefore we consider that we have confirmed reliability of the calculation.

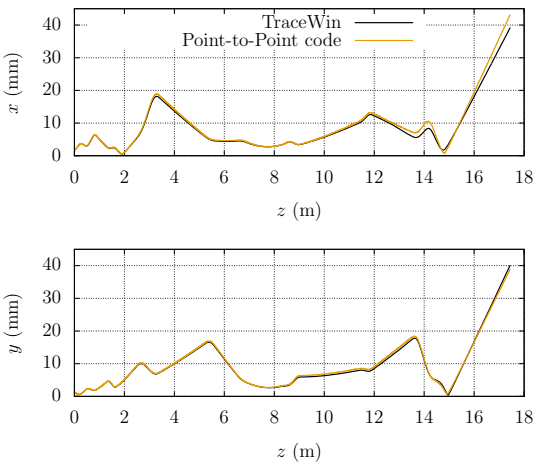

Figure 3: Comparisons of rms beam sizes from the RFQ exit to the beam dump between TraceWin and Point-to-Point code.

COMPARISONS OF MEASURED AND SIMULATED BEAM PARAMETERS

The beam operations were performed in the spring of 2024. The beam current was 116 mA and the second buncher was powered. The measured beam sizes were not agreed with simulated one. We used conversion factor from quadrupole current to magnet field gradient for perform the TraceWin simulation. We checked the factor by using the practical beam and a steering magnet before the quadrupole called

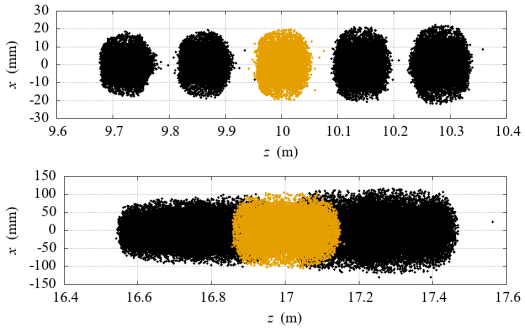

Figure 4: Bunch shapes calculated by Point-to-Point code. At $z = 10$ m, the bunches are independent, although they are overlapped downstream (at $z = 17$ m).

GtoI method [3] and the factor turned out to be slightly different. Additionally, we used hard edge field model for longitudinal distribution of the quadrupole fields, which is rectangular shape in the longitudinal direction. TraceWin calculations were performed again using calibrated quadrupole gradient and fringe field model for longitudinal distribution shown in Fig. 5 along with the calculation of hard edge with non-calibrated gradient model. Two calculations are clearly different.

The measured beam size in the summer of 2024 at specific points are shown in Fig. 6 along with the corrected calculation. The calculated beam sizes are almost the same as measured sizes. Figure 7 shows the measured and simulated twiss parameters at point A in Fig. 6. The measured twiss parameters also agreed with simulations. This indicates that the simulation reproduces the experimental facts very well. As a result, we achieved a beam duty cycle of 8.75 % with current of 119 mA using these calculated parameters.

Note that simulations in Fig. 2 and Fig. 3 are using corrected quadrupole gradient and the fringe field model.

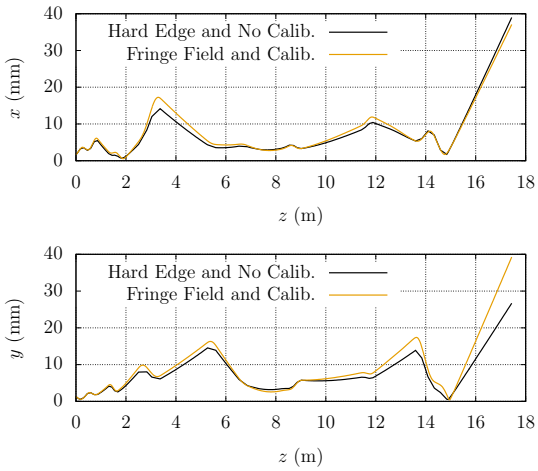

Figure 5: Difference of rms beam sizes between hard edge with non-calibrated gradient model and fringe field with calibrated gradient model.

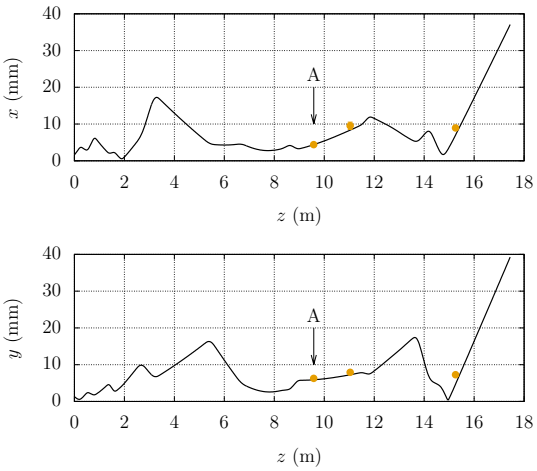

Figure 6: Comparisons between measured rms beam sizes and simulations. Orange points are measured data. Error bars are plotted but they are very small.

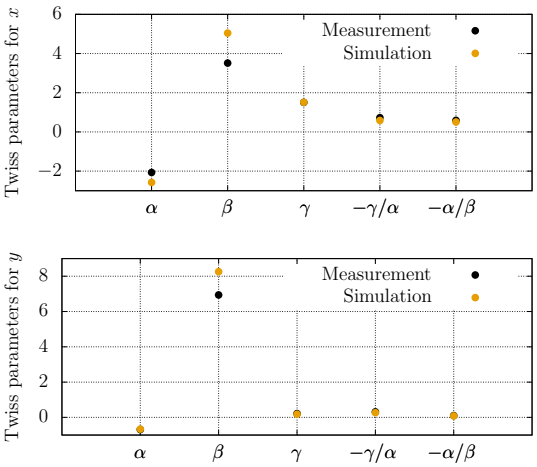

Figure 7: Measured and simulated twiss parameters at point A in Fig. 6.

WHY SIMULATIONS AGREE WITH MEASUREMENTS VERY WELL

The simulation before the RFQ is more complicated than after the RFQ. Because there are many unknown parameters such as charge distribution in the ion source, the space charge compensation factor (SCC) or so on. Space charge compensation occurs due to gas leaking from the ion source, and the details are unclear. But the beam size of the RFQ entrance section changes significantly depending on the SCC value.

Up to the RFQ section, we use TraceWin with Toutatis option [1] to calculate SCC effects. Figure 8 shows phase space profiles at entrance and exit of the RFQ with different SCC settings. In calculation A, SCC is 100 % at entrance of injection cone shown in Fig. 9 and decreases linearly to 70 % at entrance of the RFQ, whereas in calculation B, SCC is continuously 100 % from the entrance of the cone to the entrance of the RFQ. The solenoid coil settings are different in calculation A and B since beam sizes before

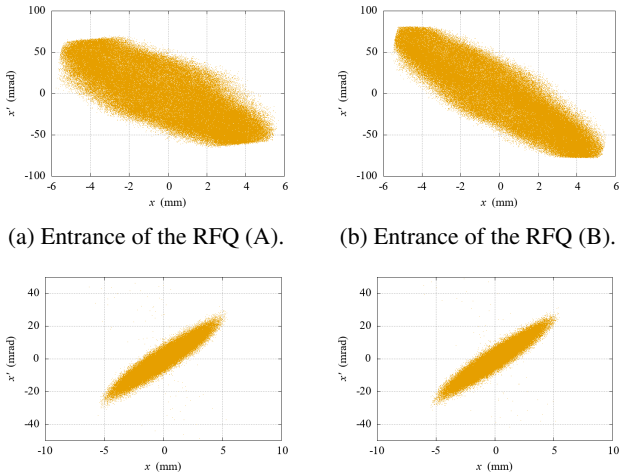

(a) Entrance of the RFQ (A). (b) Entrance of the RFQ (B).

(c) Exit of the RFQ (A). (d) Exit of the RFQ (B).

Figure 8: Phase space profiles of calculation A and B, at entrance and exit of the RFQ.

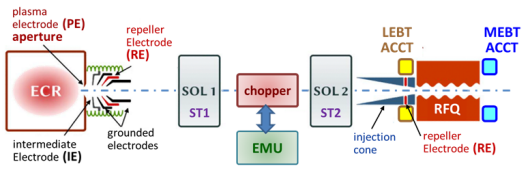

Figure 9: Schematic diagram before the RFQ.

the RFQ are different. The RFQ power is the same for the both calculations. At entrance of the RFQ, phase space plots are different as shown in Fig. 8 but at exit of the RFQ, they become to be almost the same.

Figure 10 shows TraceWin calculations from the RFQ exit to the beam dump using Toutatis calculation data as shown in Figs. 8(c) and 8(d). Although there is a clear difference in the calculation conditions between calculations A and B, the time evolution of the beam size after the RFQ shown

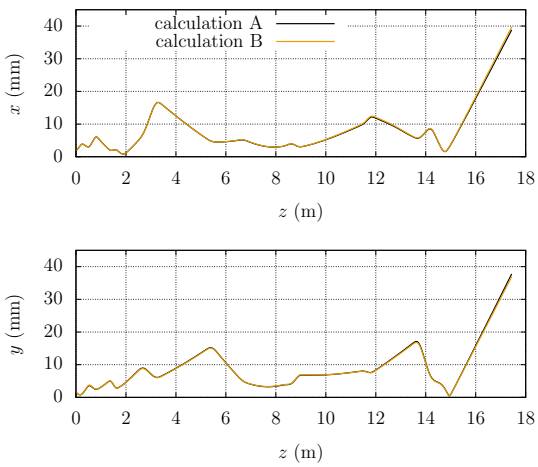

Figure 10: Rms beam sizes from the RFQ exit to the beam dump with different SCC settings. The two calculations are in almost perfect agreement.

in Fig. 10 is almost the same for both. This indicates that beam characteristics can be determined by the RF buckets of the RFQ, since the RFQ is very long at almost 10 m. The RFQ acts as if it were some kind of beam filters and then, TraceWin simulations agreed with measurements very well.

This facts is lucky for us but we have to keep investigation for beam dynamics in the injector part.

HALO CALCULATION

Even though the measured beam size agreed well with the simulation, vacuum degradation was observed at point A in Fig. 2, where the aperture is narrow. We consider this degradation comes from beam halo. Calculating halos is generally difficult because parts of the beam with widely differing intensities must be calculated simultaneously. Here, we introduce an idea to overcome this issue.

Bulk-to-Point code [4], which was developed by the author, is not a PIC code but it calculates beam induced electromagnetic field directly. It calculates the bulk-induced field instead of the field induced by a point charge, and applies it to each particle to perform tracking. Figure 11 shows relationship between the bulks and particles. The bunch is divided into m slices in the longitudinal direction and n parts in the transverse direction. Each particle is located at each segmentation corner. Each donut is the bulk and charge of the bulk can be given arbitrarily. Therefore, there is a possibility to calculate widely differing intensity parts simultaneously. There is a limited condition in Bulk-to-Point code that x-y cross section must be elliptical, but the actual cross section at the exit of the RFQ is shaped more like a diamond. Here, we describe Bulk-to-Point calculations with assuming that shape of the cross section at exit of the RFQ is elliptical.

Figure 12 shows longitudinal input profile for Bulk-to-Point code at the exit of the RFQ. m and n are set to 60 and 30, respectively. The orange lines are meant to distinguish the origin of the halo at specific points, which will be shown later. The time evolution of transverse rms beam size calculated by Bulk-to-Point code is shown in Fig. 13 along with those by TraceWin. The calculated conditions are the same as Fig. 3. The beam sizes are a little bit different and it may be

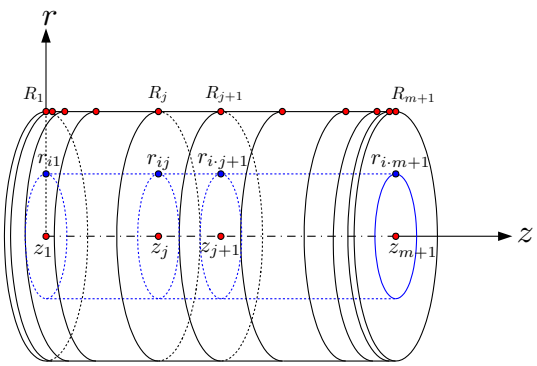

Figure 11: Bunch segmentation model used for Bulk-to-Point code.

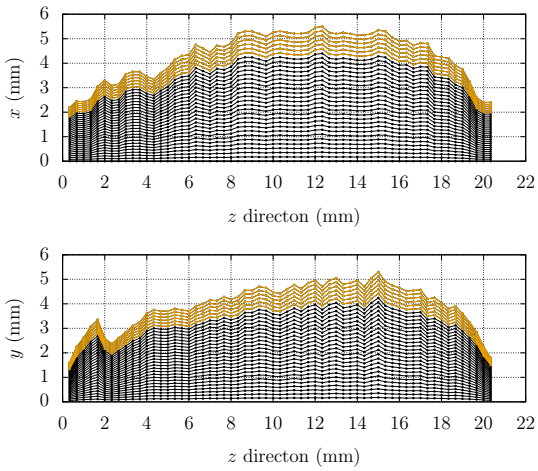

Figure 12: Initial longitudinal beam profile for Bulk-to-Point code.

caused from the assumption of elliptical cross section at the exit of the RFQ.

The transverse bunch profiles at point A in Fig. 2 calculated by Bulk-to-Point code and TraceWin are shown in Fig. 14. Halo like figures are visible in the plots of both codes. From Bulk-to-Point code calculations, halos consists of orange plots in x direction as shown in Fig. 14(a). This indicates that the halo is generated from the outer part of the bunch at the RFQ exit. Whereas in the y direction the halo originates from the whole bunch as shown in Fig. 14(c). The origin of the halo like this is considered to be very important but the mechanism of difference between Fig. 14(a) and Fig. 14(c) is currently unknown.

The charge on the outermost donut as shown in Fig. 12 is 3×10^{-5} relative to the total charge. In the LIPAc project, we are considering halos smaller than 10^{-6}. This can be achieved by dividing the outermost donut into 10 parts and leaving the inner donuts sparser. However the elapsed time for calculation takes longer. For this reason, we are planning

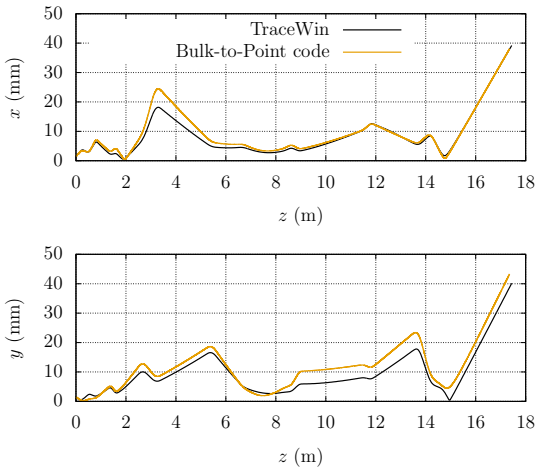

Figure 13: Rms beam sizes from the RFQ exit to the beam dump calculated by Bulk-to-Point code along with calculated by TraceWn.

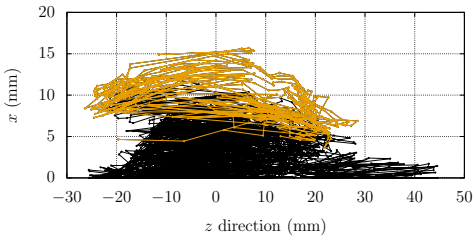

(a) x profile by Bulk-to-Point code.

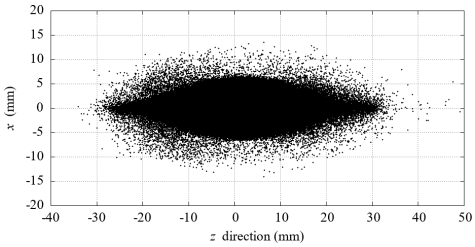

(b) x profile by TraceWin.

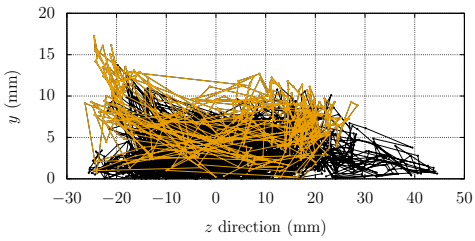

(c) y profile by Bulk-to-Point code.

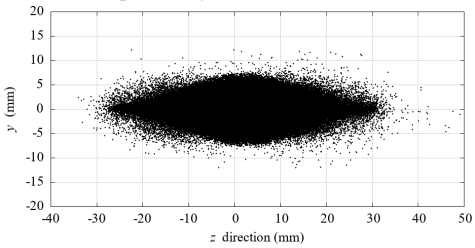

(d) y profile by TraceWin.

Figure 14: Profiles at point A in Fig. 2.

to use a supercomputer to calculate halos which consists of more smaller charge.

SUMMARY

In the LIPAc project, we perform a beam simulation in advance and determine the parameters of devices for avoiding activation or heat accidents by the high intensity beam and use TraceWin for beam tracking simulations. The benchmark test with Point-to-Point code using bunch train model for the both codes was performed and the transverse rms beam size agrees very well. Since the space charge field calculation technique is completely different for the both codes, we believe that we have confirmed the accuracy of TraceWin. Comparisons of measured and TraceWin simulated beam sizes were performed and the results agreed very well using fringe field model and corrected fields for the quadrupoles in TraceWin. We also confirmed by Toutatis simulations that the beam parameters at exit of the RFQ do not depend on the beam parameters before the RFQ but on the RF bucket conditions. Therefore, the measured beam sizes agree with TraceWin simulations very well. We consider that above methods such as pre-calculating and determining quadrupoles parameters in advance also can be applied to the SRF beam operations starting in the near future. Even though the measured beam size agreed well with the simulation, vacuum degradation was observed where the aperture is narrow. We performed by Bulk-to-Point code simulations and confirmed that halos are generated at that point. There is a possibility of simulating halo by Bulk-to-Point code but high speed computer is necessary to calculate more smaller charged halos, and now we are planning to use a supercomputer. Our team has also developed the envelope equation [5], and we plan to use this method in combination to investigate the mechanism of the halo.

ACKNOWLEDGEMENTS

This work was undertaken under the Broader Approach Agreement between the European Atomic Energy Community and the Government of Japan. The views and opinions expressed herein do not necessarily state or reflect those of the Parties to this Agreement.

REFERENCES

[1] TraceWin and Toutatis, `https://dacm-logiciels.fr/tracewin` `https://dacm-logiciels.fr/toutatis`

[2] A. Mizuno *et al.*, Nucl. Instrum. Methods Phys. Res. Sect. A. **528**, 387 (2004). `doi:10.1016/j.nima.2004.04.086`

[3] J. Hyun *et al.*, Proc. IPAC'24, Nashville, TN, May 2024, pp. 3512–3515. `doi:10.18429/JACoW-IPAC2024-THPR14`

[4] A. Mizuno, Phys. Rev. Accel. Beams 19, 024201 (2016). `doi:10.1103/PhysRevAccelBeams.19.024201`

[5] T. Ebisawa and K. Takayama, AIP Advances **13**, 045316 (2023). `doi:10.1063/5.0146071`